J Mater Sci
DOI 10.1007/s10853-014-8635-z

Flexible-structured systems made of ceramic fibers containing Pt-NaY zeolite used as CO oxidation catalysts

J. P. Cecchini · E. D. Banús · S. A. Leonardi · M. A. Zanuttini · M. A. Ulla · V. G. Milt

Received: 4 July 2014 / Accepted: 26 September 2014

Abstract Catalytic ceramic papers were developed by incorporating Pt-NaY zeolite to ceramic papers. The necessary mechanical strength was enhanced by the addition of natural borate compounds, which confer elasticity and resistance similar to those obtained using colloidal suspensions, which are the most commonly used binders. Pt-NaY zeolite was incorporated into ceramic papers either during the papermaking process or by spraying a zeolitic suspension on ceramic papers. The partial encapsulation of the faujasite by the sintering of the borate compound during the calcination step made catalytic ceramic papers less active toward the CO oxidation reaction than the corresponding traditional systems (Pt-NaY zeolite coated onto cordierite monoliths or the powder Pt-NaY faujasite). Light-off curves indicated that the activity of Pt-NaY zeolite was preserved when incorporating the zeolitic component by spray, in which case the CO oxidation reaction ran away at ca. 130 °C, and the total CO conversion was achieved at 150 °C, maintaining 100 % CO conversion for more than 90 h.

J. P. Cecchini · E. D. Banús · S. A. Leonardi · M. A. Ulla · V. G. Milt (✉)
Instituto de Investigaciones en Catálisis y Petroquímica (INCAPE), FIQ, UNL-CONICET, Santiago del Estero 2829, S3000AOM Santa Fe, Argentina
e-mail: vmilt@fiq.unl.edu.ar

J. P. Cecchini
e-mail: jpcecchini@fiq.unl.edu.ar

E. D. Banús
e-mail: edbanus@fiq.unl.edu.ar

S. A. Leonardi
e-mail: sleonardi@fiq.unl.edu.ar

M. A. Ulla
e-mail: mulla@fiq.unl.edu.ar

S. A. Leonardi · M. A. Zanuttini
Instituto de Tecnología Celulósica (ITC), FIQ, UNL, Santiago del Estero 2654, S3000AOJ Santa Fe, Argentina
e-mail: mzanutti@fiq.unl.edu.ar

Introduction

There are numerous catalytic processes through which the environmental impacts caused by both fixed and mobile sources are minimized. Many of them require the use of structured catalysts that can promote effective diffusion of heat and reactants [1]. Monolithic ceramic supports with honeycomb structure consisting of regularly arranged parallel channels have been popularized, and cordierite ($2MgO\text{-}Al_2O_3\text{-}5SiO_2$) has been commonly employed as a monolith substrate for automotive catalytic converters, mainly due to its strong thermal and physical stabilities, which offers high geometric surface area and strong thermal resistance up to 1200 °C. Ceramic monoliths occupy nearly 95 % of the catalytic converter market for automotive engines. However, honeycomb-structured catalysts present certain disadvantages, namely heaviness, poor lateral gas diffusion, and low thermal conductivity [2].

As an alternative, ceramic papers (CPs) offer the advantage of the arrangement of ceramic fibers in a flexible structure that can be easily fabricated and accommodated under different geometries. To increase the retention of inorganic compounds during the synthesis of the catalytic CPs, a combination of anionic and cationic polyelectrolytes is used. The incorporation of binders during the paper manufacturing allows obtaining structures easy-to-handle in practical use, which should be rolled and folded without breaking. To obtain catalytic papers, the catalyst can be deposited on a finished CP or catalytic particles can be

Published online: 09 October 2014

immobilized in the fibrous network if they are added during the paper preparation. Catalytic CPs have been used for different reactions such as the solid oxide fuel cell (SOFC) [3, 4], the steam reforming of biodiesel fuel [5], the oxidative dehydrogenation of ethane [6], methane steam reforming [7], methanol reforming [8], reduction of 4-nitrophenol [9], NO_X reduction [10, 11], for toluene removal [12], and catalytic soot removal [13].

One important challenging feature in the synthesis of these catalytic CPs is their mechanical resistance. Almost all preparations reported include the use of colloidal suspensions of Al_2O_3, CeO_2, or ZrO_2 as binders that join ceramic fibers by sintering after a calcination step [3–6, 8, 11, 14]. Recently, we reported the use of a novel type of compounds, borates, as binders [15]. In this report, the calcium borate compounds tested were found suitable as ceramic binders, and the mechanical properties of CPs varied significantly depending on the calcium borate used as well as on the calcination temperature. Although none of the borates used melted under calcination conditions, individual particles began to sinter as the calcination temperature increased, thus joining ceramic fibers and giving the CPs the necessary mechanical strength properties. Ceramic papers prepared using nobleite and colemanite as binders exhibited the highest paper strength values after calcination at 700–750 °C. However, this value was limited to the maximum temperature that NaY zeolite resists without any damage to the faujasite structure. In this way, if the calcination temperature was limited to 650 °C, then the anhydrous ulexite provided better strength and elasticity. In comparison with colloidal suspensions, borates have the advantage of being less expensive and easily obtained [16].

For the oxidation of CO to CO_2, many catalytic materials have been tested, and the catalysts most widely used contain noble metals, for example, Pt/CeO_2 or Pt/CeO_2-ZrO_2 [17], $Pd/FeMnO_3$ [18], Pd/Mn_2O_3 [19], and Au nanoparticles deposited over CeO_2, TiO_2, Al_2O_3, ZrO_2, ZnO, or MgO [20]. Noble metals exchanged or deposited over different types of zeolites have also been studied [21, 22], as well as non-noble metals such as CuO-CeO_2-ZrO_2 over Al_2O_3 [1], CuO-CeO_2 catalysts supported on SiO_2 [23], or $Co_3O_4 + CeO_2/SiO_2$ [24]. Other authors proposed the use of nanoalloys as Pd-Au for the low-temperature oxidation of CO [25]. Nevertheless, these catalysts were tested as powders. For mobile sources and for several stationary ones, powder catalysts cannot be used and, instead, structured catalysts are necessary. As mentioned above, the structures most commonly used for the synthesis of structured catalysts are monoliths, in addition to metallic [2, 26] or ceramic [27, 28] foams. For the CO oxidation, different structured catalysts, such as Au/TiO_2 supported on ferritic stainless steel monoliths [29], Cu, Ce/mordenite coatings on FeCrAl-alloy corrugated foils [30], $Pd/MMnO_x$ (M = Co, Ni, Fe, and Cu) over cordierite monoliths [31], Au/CeO_2 supported on metallic foams [32], Pt/SnO_2 over alumina foams [2], and Pt/Al_2O_3 supported on stainless steel foams [33], have also been used as well as a wire mesh with a CuO-CeO_2/zeolite film [34].

All these structured systems are rigid. However, the elasticity and the flexibility of the silicalite films grown on the surface of a magnetoelastic material have recently been reported [35], which provided insight into the design of zeolite permselective membranes. As a novel alternative, catalytic CPs were developed in the present work by incorporating Pt-NaY zeolite to CPs. The mechanical strength necessary to handle them was achieved by adding borate compounds. Their performance for the CO oxidation reaction was compared with the catalytic activity shown by both the conventional structured catalyst (Pt-NaY over cordierite monolith) and the powder catalyst. Considering that over 90 % of CO is produced from both gasoline powered engines [36] and from many industrial processes, the flexible-structured catalysts here presented are interesting for industries as well as for vehicles, since they can be adapted to mobile or fixed reactors.

Experimental

Powder catalysts

NaY zeolite (Si/Al atomic ratio = 2.8) was prepared by hydrothermal synthesis. The gel, molar composition of which was H_2O:SiO_2:Na_2O:Al_2O_3 = 20:1:0.5:0.083 (Si/Al atomic ratio = 6), was prepared starting from NaOH, H_2O, $Na_2Al_2O_4$, and colloidal SiO_2 (Ludox, 40 wt% of SiO_2). After annealing at room temperature for 24 h under stirring, the gel was placed inside an autoclave that was hermetically sealed and kept in an oven at 100 °C for 24 h. Then, zeolite crystals were filtered, washed with abundant distilled water, and dried in an oven at 100 °C overnight. The zeolite thus synthesized was called NaYZ.

Platinum was incorporated into NaYZ by ionic exchange in an aqueous solution of $Pt(NH_3)_4(NO_3)_2$ by stirring for 24 h at room temperature to obtain the desired loading (the amount of $Pt(NH_3)_4(NO_3)_2$ contained in the aqueous solution, which was calculated to obtain 1 wt/wt% of Pt with respect to the mass of zeolite). After filtration, the powder was dried in an oven at 120 °C overnight. The solid thus obtained was called Pt-NaYZ.

Rigid-structured catalyst: Pt-NaY zeolite coated onto cordierite monoliths

Cordierite honeycomb monoliths (Corning, 400 cps, 0.17-mm average wall thickness) were used as rigid substrates.

Portions of monoliths containing 64 channels were used in these preparations, their dimensions being approximately 1 cm × 1 cm of section and 2 cm long. NaY zeolite was incorporated into cordierite monoliths by hydrothermal synthesis assisted by seeding, for which the outer faces of the cordierite monoliths were covered with a Teflon tape so that the depositions were performed only inside the channels.

The cordierite support was seeded with NaY zeolite crystals prior to the hydrothermal treatment by dipcoating in a 2 wt/wt% zeolite crystals suspension. Afterward, the seeded support was dried in air for 30 min. The seeding process was repeated twice.

The composition of the synthesis gel was the same as that used for the preparation of NaY zeolite. This gel was aged by stirring for 24 h at room temperature, and the synthesis was carried out at 100 °C for 24 h. The support with the channels in vertical position was fixed inside a Teflon vessel together with the aged synthesis gel, leaving a void of 2 cm. The vessel was transferred to an autoclave which was then placed in a stove for the hydrothermal treatment. After the treatment, the vessel was cooled, and the sample was withdrawn from the autoclave, washed in water, kept in an ultrasonic bath for 10 min to remove weakly bonded material, and finally dried at 100 °C overnight. The remaining liquid phase from the synthesis was filtered, and the crystals produced were recovered. In order to increase the gain of zeolite over cordierite, the process was repeated. It should be remarked that no template agents were used in the procedure. The structured catalyst thus obtained was denoted as NaYZ-M.

The NaY zeolite-coated monolith (NaYZ-M) was immersed in an aqueous solution of $Pt(NH_3)_4(NO_3)_2$ and stirred for 24 h at room temperature to obtain the desired loading (1 wt/wt% of Pt with respect to the mass of zeolite) after which it was dried in an oven at 120 °C. The structured catalyst thus obtained was denoted as Pt-NaYZ-M.

At the end of the synthesis process described above, the monoliths were weighed, and the content of Pt-NaYZ was determined to be 160 mg (average value).

Flexible-structured catalyst: Pt-NaY zeolite incorporated into ceramic papers

The papermaking technique developed by Ichiura et al. [37] with a dual polyelectrolyte retention system was used for the preparation of NaY zeolite-containing papers, which implied the use of cationic and anionic polymers. Two kinds of fibers were employed, cellulosic and ceramic ones, which after calcination led to the formation of CPs suitable for high-temperature applications. In order to produce easy-to-handle papers, a borate compound was added as binder during their manufacturing.

Refractory ceramic fibers (RCF, 50 wt% SiO_2, 48 wt% Al_2O_3, and 2 wt% impurities) were obtained from a ceramic insulation from CARBO. The fibrous mat was dispersed in tap water, and the fibers were separated from low slenderness particles by an elutriation process. The yield in fibers was around 50 %, with an average fiber length of 660 μm and an average diameter of 6 μm. Cellulosic fibers, from a dry commercial, bleached softwood Kraft pulp, were re-wetted for at least 24 h and dispersed by a standard disintegrator before use. Their characteristics (3 mm in length and ribbon shape with an average width of 30 μm) allowed for the mat formation during the CP preparation.

The cationic polymer was polyvinyl amine (PVAm) (Luredur PR 8095) from BASF, with molecular weight of 4.10^5 g mol^{-1} and charge density of 4.5 meq g^{-1}, and the anionic polymer (A-PAM) was from AQUATEC, with molecular weight of 10^4–10^5 g mol^{-1} and charge density of 2.7 meq g^{-1}. To prepare the CP, under gentle agitation, 10 g of ceramic fiber, 1.50 g of cellulose fiber, 3.12 g of anhydrous ulexite, and 66 ml of PVAm solution (1 g l^{-1}) were incorporated into 1000 ml of NaCl solution (0.01 N). After 3 min of slight stirring, 42 ml of A-PAM polymer solution (0.4 g l^{-1}) was added. From this suspension, a handsheet was formed by the SCAN standard method [29] but using tap water (180 mS) and applying the double of the standard pressing pressure (37.5 kPa). The wet sheet was dried under atmosphere where the temperature and the relative humidity were controlled (23 °C and 50 % RH) for 24 h and finally calcined in air for 2 h at 650 °C. According to previous results [15], this temperature was chosen in order to preserve zeolite structure. The final CPs as prepared consisted of circular sheets with 160 mm diameter and 2.5 mm thickness.

The Pt-containing zeolite was incorporated into these ceramic structures in different ways. One method consisted in the incorporation of the prepared powder zeolite (Pt-NaYZ) during the papermaking procedure, as shown in Fig. 1. First, Pt-NaYZ was milled, and 1.0 g of the fraction of particles that passed through the 80-mesh sieve was dispersed in water of 180 mS and stirred for 5 min under ultrasound (aqueous Pt-NaYZ suspension). The wet paper containing Pt-NaYZ was first dried under controlled atmosphere, as previously described, and then calcined at 650 °C for 2 h. The catalytic CP thus obtained was denoted as Pt-NaYZ-P and contained 0.05 mg of Pt-NaYZ/mm^2 catalytic ceramic disk, considering 100 % retention.

Another method employed was to incorporate Pt-NaYZ into the CP. To this end, an aqueous Pt-NaYZ suspension, as previously described, was used to spray the zeolite all around the CP disks, on both sides. The catalytic CP thus obtained was denoted as Pt-NaYZ-PS and contained 0.04 mg of Pt-NaYZ/mm^2 catalytic ceramic disk.

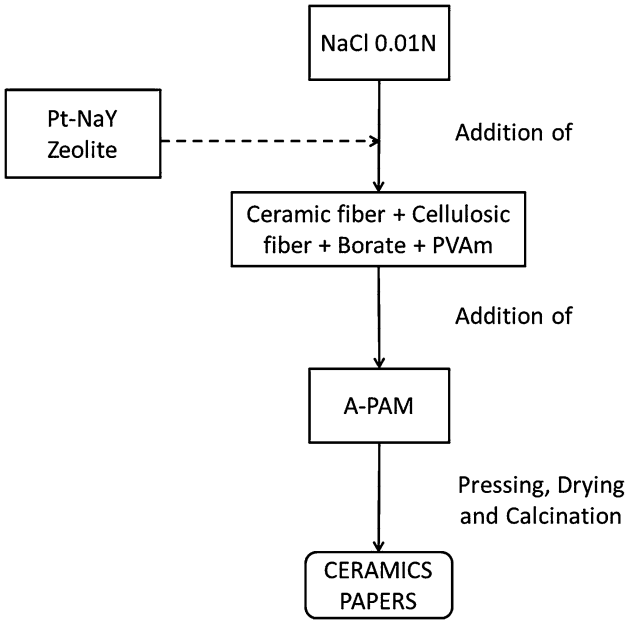

Fig. 1 Scheme of the preparation of ceramic papers

Characterization

Crystalline phases were determined on a Shimadzu XD-D1 instrument with monochromator using CuKα radiation at a scan rate of 1 ° min^{-1}, with the range of $2\theta = 5°$ to 50°. In the case of powders, they were compressed in the sample holder, whereas for both CPs and monoliths, a void sample holder designed for this analysis was used. For CPs, pieces of about 2 cm × 2 cm were cut and supported in the special sample holder, whereas for the cordierite monolith, a plaque was obtained after cutting the perpendicular walls of a piece of monolith and then, it was placed in the sample holder. The software package of the equipment was used for the phase identification from the X-ray diffractograms.

The morphologies of both monoliths and CPs were studied using a ZEISS instrument SUPRA 40 model, which was operated at 20 kV as acceleration voltage. The apparatus possesses an EDS detector, Oxford Instruments, for EDX semiquantitative analysis, with a FEG (Field Emitter Gun) electron source. Samples were glued to the sample holder with Ag painting and then coated with a thin layer of Au in order to improve the images.

The tensile strength and stiffness of CPs were determined using an INSTRON 3344 universal tester equipped with a 10-N load cell. The standard procedure as per TAPPI T 494 om-01 for cellulosic papers was followed.

The air resistances of papers were determined using a Gurley apparatus. The standard procedure was followed, according to the TAPPI T 460 norm. The results of this test were reported as seconds per 100 ml, called as Gurley seconds, which referred to the time required for air to flow through a cylinder of 3.14 cm^2 section (this section value is half the one commonly used in the Gurley test for cellulosic papers).

Catalytic activity

The catalytic oxidation of CO was carried out in a conventional continuous flow quartz reactor operating at atmospheric pressure. The outlet gas compositions were analyzed using a Shimadzu GC-2014 chromatograph (equipped with TCD detector and 5A zeolitic column). In order to calculate CO conversion, the initial CO area (A°) of the chromatogram was obtained by analyzing the feeding stream before passing through the reactor. At other temperatures with the reactant mixture passing through the reactor, the CO areas of the chromatogram were denoted as A.

Equation 1 was used to calculate CO conversion at any temperature:

$$X_{CO}(\%) = 100(A^\circ - A)/A^\circ \quad (1)$$

.

Light-off curves

The light-off curves for CO oxidation were obtained with a constant W/F ratio of 2.5 (i.e., 2.5 mg min ml^{-1}, where W is the Pt-NaYZ mass and F is the total gas flow), which was maintained by changing the total gas flow in order to make a suitable comparison for the different structures. In the case of the powder solids, 125 mg of Pt-NaYZ was loaded to the reactor, whereas for catalytic monoliths, a piece of 1 cm × 1 cm of section and 2-cm length, coated with the 168 mg of Pt-NaYZ, was loaded in the evaluation reactor to check their activity. In the case of CPs, 13 stacked disks 16 mm in diameter were loaded into the reactor. In the case of catalytic CPs, considering the zeolitic content as previously described in "Flexible structured catalyst: Pt-NaY zeolite incorporated into ceramic papers" section, Pt-NaYZ-P loaded into the evaluation reactor contained 130 mg of Pt-NaYZ, whereas for Pt-NaYZ-PS, the corresponding value was 100 mg of Pt-NaYZ.

The way in which the different catalysts were loaded into the catalytic reactor is better described in Fig. 2. The powder catalyst (Fig. 2a) was loaded over quartz wool, whereas in the case of the monolithic catalyst (Pt-NaYZ-M, Fig. 2b), it was placed with quartz wool all around in order to force the gas flow through the monolith channels. Catalytic CP disks (e.g., Pt-NaYZ-P, Fig. 2c) were stacked over quartz wool.

Before the catalytic tests, each structured or powder catalyst was pretreated as follows: (i) calcination at 300 °C for 12 h in air, with a heating rate of 3 °C min^{-1}, (ii)

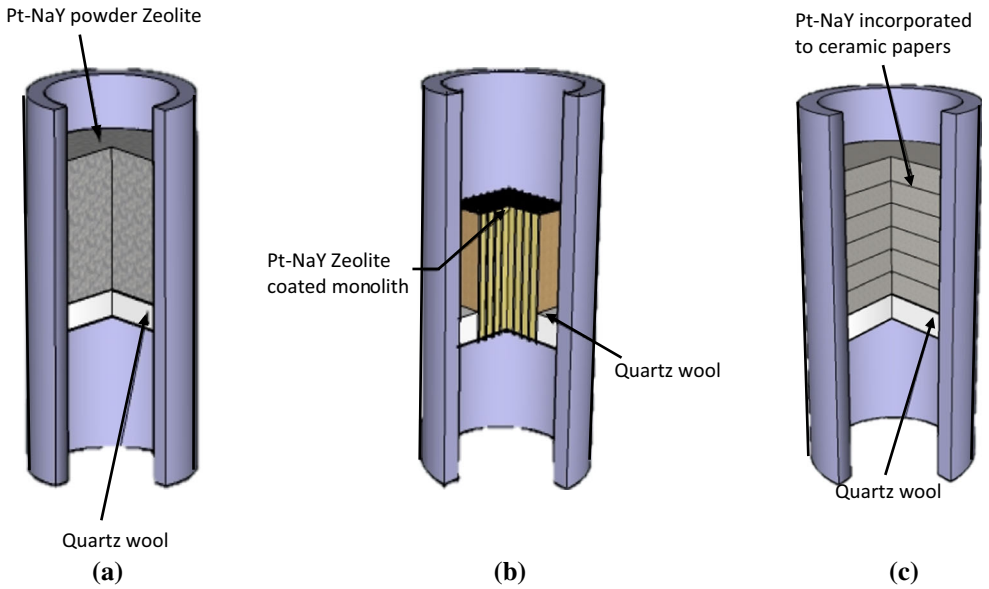

Fig. 2 Catalysts' disposal for catalytic evaluation. Pt-NaYZ (**a**), Pt-NaYZ-M (**b**), and Pt-NaYZ-P (**c**)

sweeping with He flow at 300 °C during 45 min in order to remove remaining air, (iii) reduction at 300 °C in H_2/He stream (1:1), (iv) cooling in He flow up to 50 °C, and (v) heating under reactant mixture (0.5 % CO + 10 % O_2, diluted in He) from 50 to 150 °C at a heating rate of 1 °C min^{-1} and maintaining this latter temperature during 2 h (activation under reaction conditions). After this pre-treatment, catalysts were cooled down to 50 °C under He flow. Light-off curves were obtained by heating the pre-treated catalyst under the reactant mixture from 50 to 300 °C, with a heating rate of 1 °C min^{-1}.

Long-term runs

To check the stability of the catalysts, long-term experiments were performed. To this end, new batches of catalysts were prepared and tested, as previously described. After obtaining light-off curves, the catalysts were maintained at 150 °C for more than 90 h, while continuously monitoring the activity.

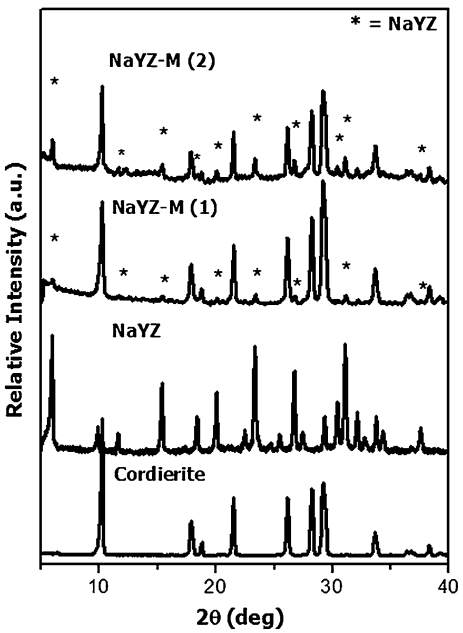

Fig. 3 XRD patterns of NaY zeolite coated onto cordierite monoliths

Results and discussion

Pt-NaY zeolite coated onto cordierite monoliths

Figure 3 shows XRD patterns of cordierite monoliths coated with NaY zeolite (NaYZ-M), after one [NaYZ-M (1)] or two [NaYZ-M (2)] consecutive hydrothermal syntheses and also, the corresponding diffractograms of both NaYZ and the bare cordierite monolith. All signals observed for NaYZ correspond to the faujasite structure (JCPDS # 39–1380). After the one-synthesis step, the amount of NaYZ deposited on the cordierite monolith walls was 3.5 wt/wt% ± 1.8, and after the two-synthesis steps, it increased up to 16.2 wt/wt% ± 3.9, values that are averages of eight batches. The higher content of NaYZ onto the monolith walls after two syntheses can be clearly observed through the more intense signals in the corresponding XRD diffractogram.

Figure 4 shows SEM micrographs of Pt-NaYZ-M, where the zeolitic coating deposited on the cordierite

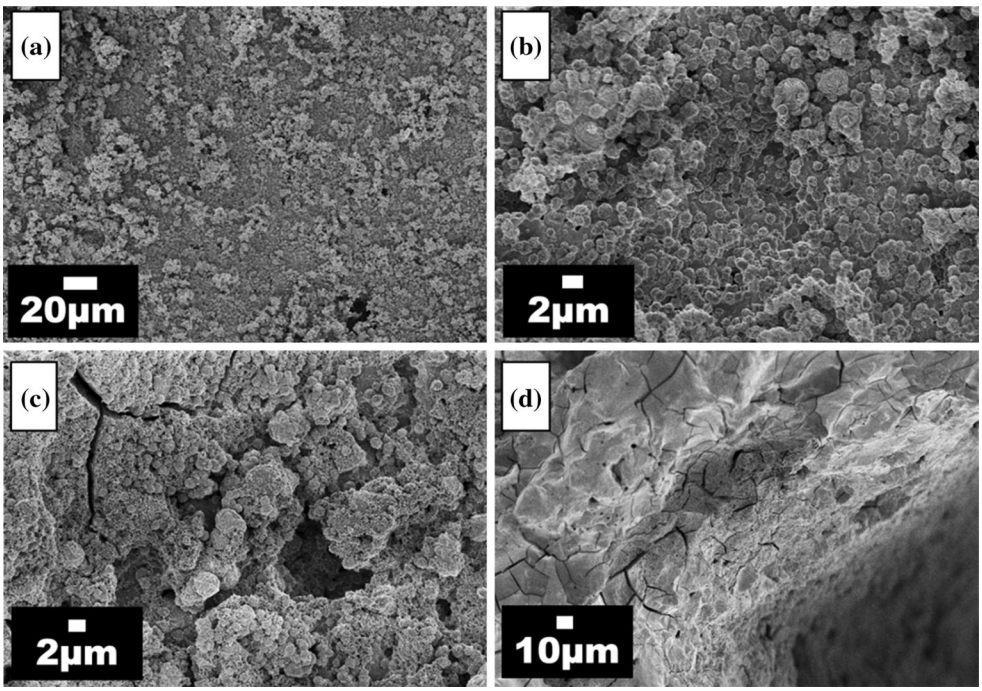

Fig. 4 Morphology of Pt-NaY zeolite coated onto cordierite monoliths, Pt-NaYZ-M (**a**), front views in detail (**b**, **c**), and cross-sectional view (**d**)

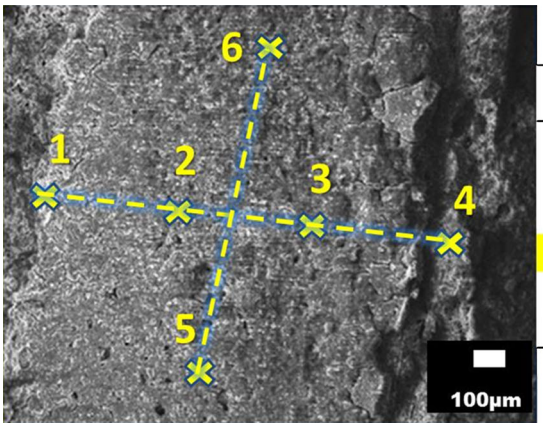

Fig. 5 EDX analysis of Pt-NaYZ-M. 1–6 marks indicate points of analysis, with their corresponding atomic ratios being shown in the table attached

Sample	Si/Al) atomic ratio	Pt/Al) atomic ratio
1	2.92	0.04
2	2.69	0.03
3	3.57	-
4	1.45	-
5	2.50	-
6	3.24	0.04

monoliths after two consecutive hydrothermal syntheses is observed. The high weight gained was achieved after the two-synthesis steps produced abundant deposits of zeolite, which deposited not only on the monolithic walls but also inside cordierite macropores. The faujasite appears forming aggregates of ca. 1 μm, with rounded edges. A cross-sectional view shows that it is difficult to distinguish the interface between the zeolitic coating and the monolith, probably due to the fact that faujasite grows inside cordierite macropores.

The analysis by EDX (Fig. 5) in different sectors of a channel indicated that the Si/Al atomic ratio varied between 2.5 and 3.6. The zone denoted by "4" shows a lower value (1.5), which corresponded to the cordierite support produced when cutting the transversal monolithic walls. Pt could be detected in only some of the analyzed zones, probably due to the small amount in which it was incorporated (1 wt/wt% with respect to NaYZ).

The adherence of the zeolitic coating was determined by ultrasound, immersing the monolithic pieces in water. After 30 min of treatment, an average value of 85 % of NaYZ was retained on the monolithic wall, which is consistent with reported values [36].

Pt-NaY zeolite incorporated into ceramic papers

Figure 6 shows SEM micrographs of ceramic papers prepared without zeolite addition (CP). An open structure formed by ceramic fibers linked by borate particles can be observed. After calcination at 650 °C, borate particles

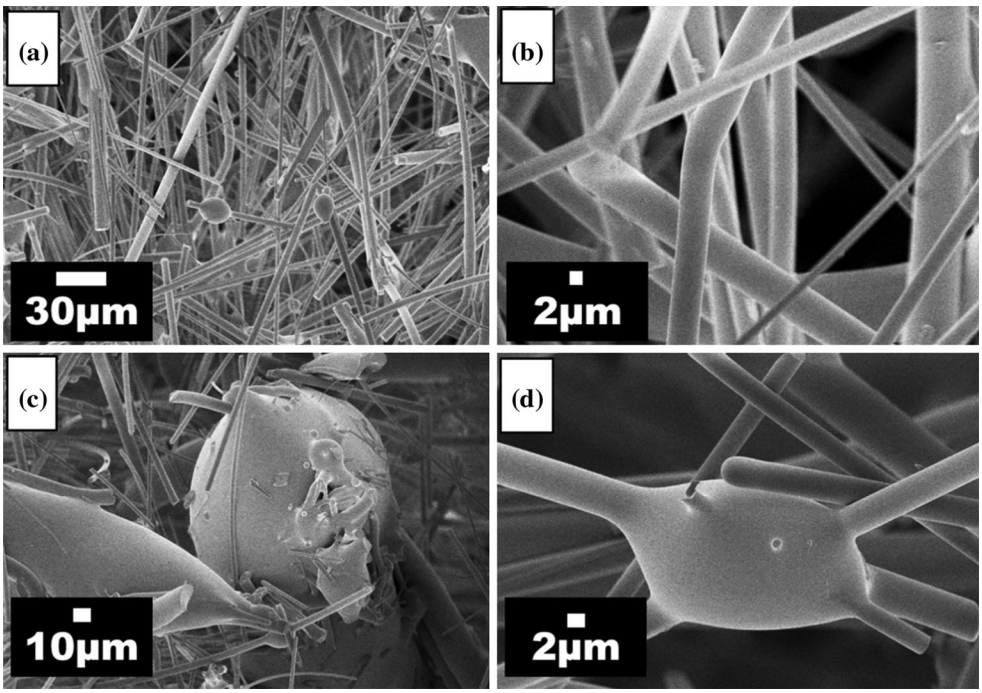

Fig. 6 Effect of borates as binders of ceramic fibers. CP morphology (**a**), closer view of ceramic fibers (**b**), and detail of ulexite particles joining ceramic fibers (**c**, **d**)

begin to sinter, acting as binders for the ceramic fibers and notably enhancing the paper's mechanical properties. Since ulexite crystals incorporated during paper manufacturing were of size <125 μm (minimum size that could be sieved), in the calcined CP, a variety of borate particle sizes are observed, ranging from ca. 1 to 100 μm. Nevertheless, the majority of ulexite particles are ca. 10 μm or less.

Figure 7a, c shows a general view of the zeolitic CP obtained after the addition of Pt-NaYZ during the papermaking process (Pt-NaYZ-P). As previously observed for CP, borate particles appear in Pt-NaYZ-P joining fibers. A closer view (Fig. 7b, d) shows zeolitic aggregates deposited both on ceramic fibers and borate particles. From Fig. 7b, it can be seen that zeolitic particles <1 μm have a similar morphology to that deposited onto monolith walls. In order to confirm that the zeolite structure is preserved after the papermaking process, XRD analyses were carried out. Nevertheless, under the preparation conditions here reported, neither ceramic fibers nor zeolitic material could be detected. In previous studies, when preparing catalytic CPs with higher NaY zeolite loadings and in the absence of a binder, it was also found that both ceramic fibers and the anhydrous ulexite were amorphous, but the crystalline structure of the NaY zeolite could be detected [12, 13, 15].

The chemical composition estimated from EDX results (Fig. 8a) indicated that for CP, when focusing on ceramic fibers, the Si/Al atomic ratio was close to unity (Table 1), which agrees with the theoretical composition of ceramic fibers (0.9).

In the case of Pt-NaYZ-P, when focusing on the small zeolitic aggregate deposited on ceramic fibers (Fig. 8b), the Si/Al atomic ratio (Table 1) slightly increased from 1.1 to 1.3 due to the presence of zeolite, for which the Si/Al atomic ratio was 2.8. On the other hand, when focusing on borate particles containing Pt-NaYZ dispersed on top (Fig. 8c), the Si/Al atomic ratio markedly increased up to 2.9, value that corresponds to Pt-NaYZ. Although boron could not be detected by this method, it was possible to detect the calcium coming from the ulexite only. In addition, the higher value of the Na/Al atomic ratio (2.3) is associated with the presence of ulexite. Even though the presence of zeolite could be detected, it was not possible to detect Pt, given its low concentration.

As CPs constitute soft structures, mechanical properties are important parameters to characterize them. With the aim of obtaining ceramic structures easy-to-handle, ulexite was added as binder, considering previous results [15]. From the INSTRON apparatus, a typical curve was obtained when plotting tensile load against elongation, and two parameters were obtained from these plots: the breaking load (BL, N), and the elastic module (EM, MPa).

Figure 9 shows Tensile Index (TI) values, expressed as

$$\mathrm{TI}\ (\mathrm{Nm\ g^{-1}}) = \frac{\mathrm{BL}\ (\mathrm{N})}{G\ (\mathrm{g\ m^{-2}})\ W\ (\mathrm{m})} \qquad (2)$$

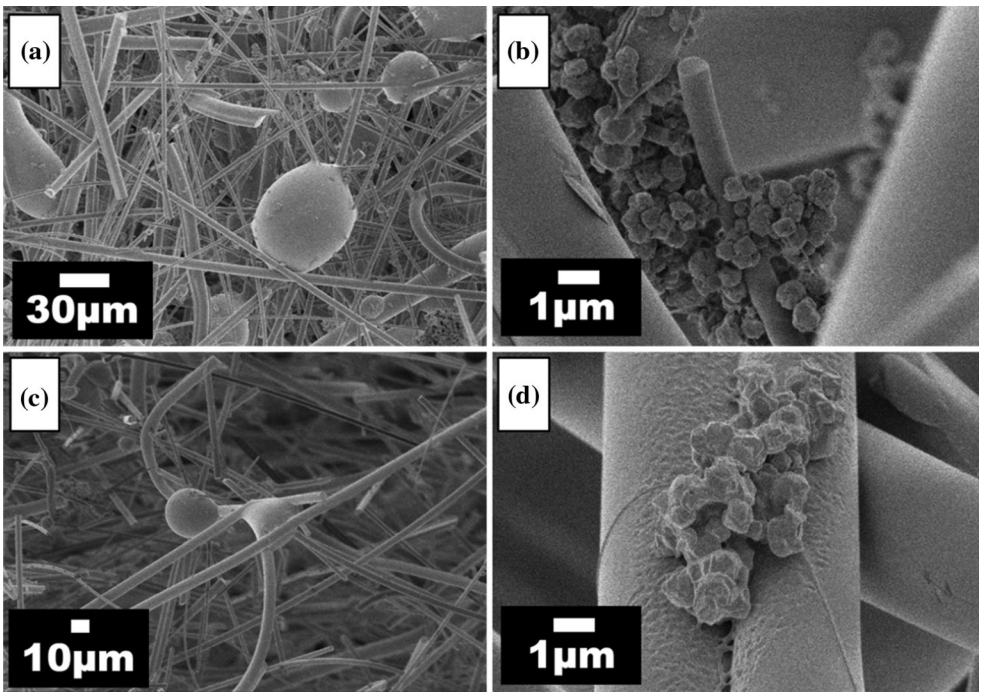

Fig. 7 Morphology of the catalytic ceramic paper (Pt-NaYZ-P) showing zeolitic aggregates (**a**, **c**). Closer views (**b**, **d**)

where G is the Grammage (weight per surface unit), and W is the paper strip width (m). At least five measurements were carried out, and the corresponding average values are here reported. The error bar associated with each measurement indicates the high variability obtained, which originated because, during these tests for CPs, failure does not occur as a "clean rupture," i.e., tensile loads exist beyond the elongation corresponding to maximum load, which indicates that, instead of individual fiber break, many fibers are pulled out during the rupture [15].

The TI value of CP is close to 0.37 N m g^{-1}, which corresponds approximately to half of the one reported for commercial CPs (*CeraTex® 3170 Ceramic Fiber Paper*), and the addition of zeolite to the CP structure decreases this value. However, differences in the TI values for NaYZ-P and Pt-NaYZ-P are negligible if considering the error bar. Even though these values are low, these structures allowed rolling, folding, and manipulating. For the sprayed sample (Pt-NaYZ-PS), the TI value is even lower (0.063 N m g^{-1}), but this sample could also be very easily handled.

The elastic modulus was obtained from the linear portion of the curve at the beginning of the test, using Eq. 3,

$$\text{EM (MPa)} = \frac{10^{-6}\ F\ (\text{N})/S\ (\text{m}^2)}{\Delta L\ (\text{m})/L\ (\text{m})} \tag{3}$$

where F is tensile load, S is paper section calculated as the probe width multiplied by paper thickness, ΔL is elongation, and L is the distance between the testing grips. High tensile index and low elastic module (high elasticity) are the desired characteristics of a CP.

For CP, the elastic modulus obtained was 23.3 MPa, and after the incorporation of zeolite, it decreased to 8.5 MPa for Pt-NaYZ-P. The value obtained for NaYZ-P was a bit lower than that of Pt-NaYZ-PS. These results indicate that after the incorporation of the zeolitic component, a more elastic structure is obtained. Compared to cellulosic papers, these values are notoriously smaller (for a low-quality cellulosic paper, the elastic modulus is 1200 MPa). Therefore, the CPs here reported are very flexible structures in comparison with the cellulosic papers.

It has to be pointed out that the high variability in values has originated from the fact that tests standardized for cellulosic papers are being applied to CPs. Also, heterogeneities in the CP composition could affect the reported values. However, in spite of these disadvantages, the method applied allowed us to quantify the mechanical properties of CPs.

Table 2 shows air resistance values determined using the Gurley method. It can be observed that all the values obtained are close to 7×10^{-3} mol s^{-1} m^{-2} Pa^{-1} and that they are very low compared to the one corresponding to a zeolitic paper prepared only with cellulosic fibers and without the addition of binder (7×10^{-2} mol s^{-1} m^{-2} Pa^{-1}). This indicates that CPs are open structures, with high porosity originating from the burning of the cellulosic fibers during the calcination process, as observed by SEM (Fig. 6).

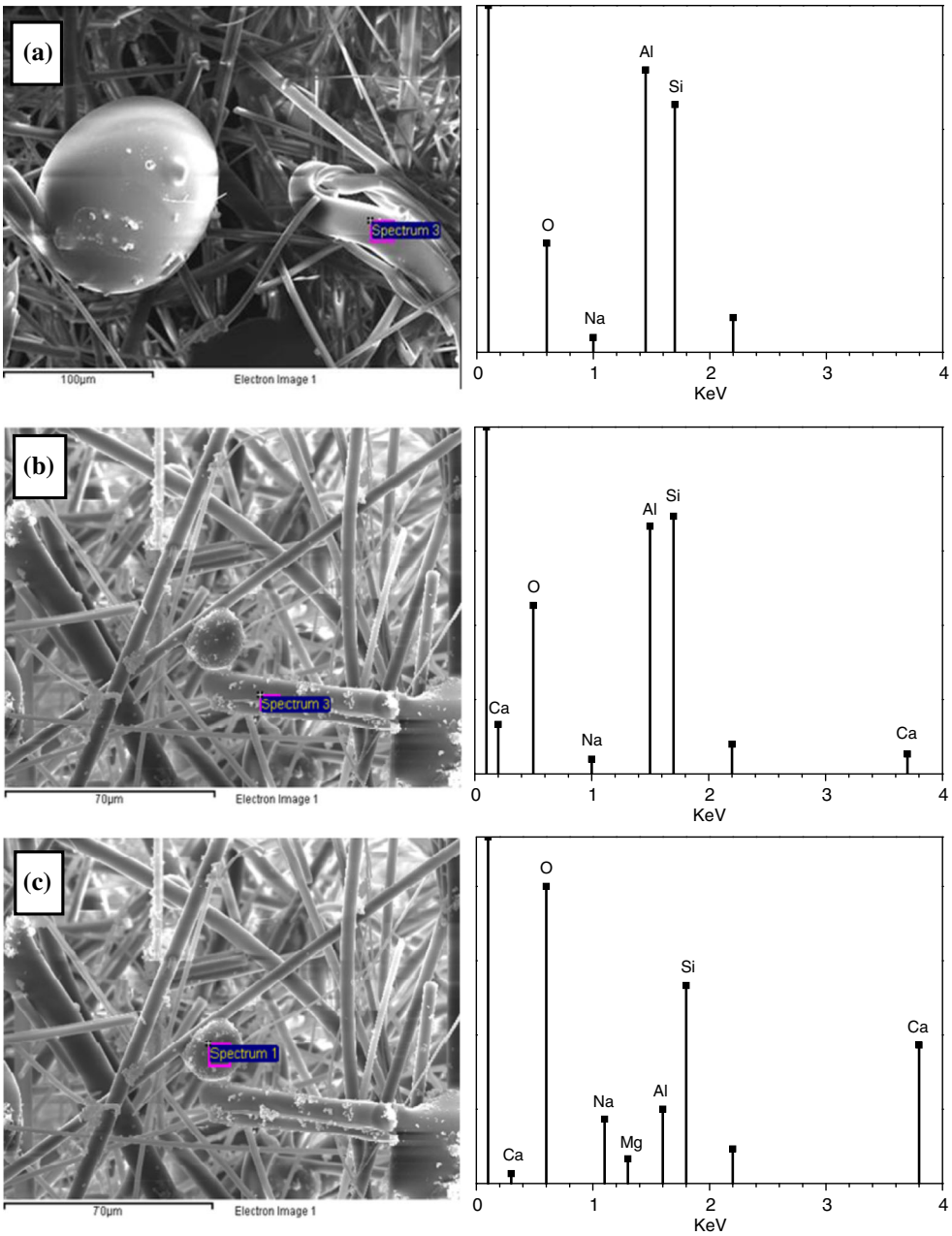

Fig. 8 Chemical composition (EDX) of ceramic papers: **a** bare CP, **b** and **c** Pt-NaYZ-P, with marked different points where the corresponding EDX spectra were acquired

Table 1 EDX analysis–atomic ratios

Compound	Si/Al	Ca/Al	Na/Al
Ceramic fibers	1.1	0.01	0.1
Ceramic fibers/zeolite NaY	1.3	0.05	0.1
Anhydrous ulexite/zeolite NaY	2.9	2.6	2.3

CO oxidation tests

Figure 10 shows the catalytic activity for CO oxidation for the prepared catalysts (Pt-NaYZ, Pt-NaYZ-M and Pt-NaYZ-P). The powder zeolite (Pt-NaYZ) exhibits a sigmoid CO conversion profile, in which the reaction ran away from 130 °C onwards, reaching 100 % CO conversion at 150 °C. Following the same trend, the profile exhibited for Pt-NaYZ-M, where zeolite appears coating the monolith walls, is very similar to that observed for the powder zeolite. This means that under these conditions, the monolithic catalyst is as active as the powder catalyst, in addition possessing the advantages for practical applications of a structured catalyst.

However, when testing the catalytic activity of the CP-containing zeolite (Pt-NaYZ-P), a notable shift to higher temperatures is observed for this structured catalyst in

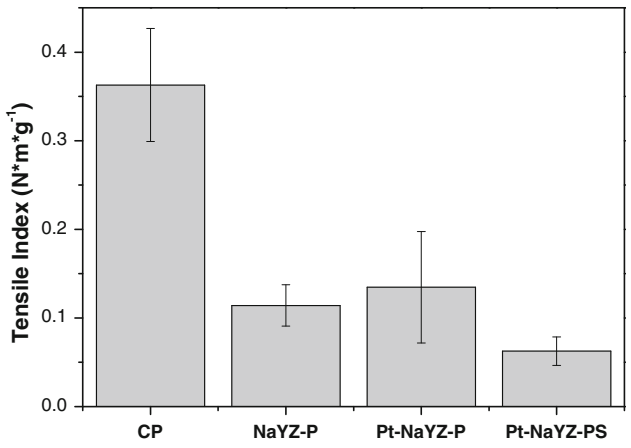

Fig. 9 TI values of bare and containing NaY zeolite ceramic papers. Values were determined using Eq. 2 from the corresponding tensile load against elongation plotting. Variation of values when analyzing at least five probes are indicated by the *error bar*

Table 2 Permeability of ceramic papers

Sample	Air resistance × 10^3 (mol s^{-1} m^{-2} Pa^{-1})[a]
CP	5.7
NaYZ-P	5.7
Pt-NaYZ-P	7.1

[a] Gurley method

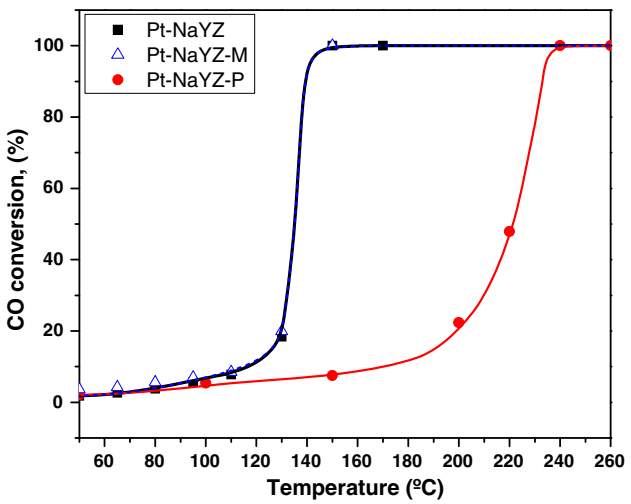

Fig. 10 Light-off curves of Pt-NaY zeolite as powder, coating the cordierite monolith or being incorporated into ceramic papers during the papermaking process

comparison with the powder zeolite (Pt-NaYZ) or the monolithic catalyst (Pt-NaYZ-M). In spite of being less active than Pt-NaYZ or Pt-NaYZ-M, Pt-NaYZ-P is more active than the corresponding papers prepared without the addition of faujasite, as the blank tests for CP indicated.

According to the SEM micrographs (Fig. 7), the partial encapsulation of the active material due to ulexite sintering could be happening. In order to gain further insight into this phenomenon, closer micrographs were acquired. Figure 11 shows the SEM pictures of Pt-NaYZ-P where this partial encapsulation effect is clearly shown. In fact, ceramic fibers with NaYZ particles covered with the sintered binder can be observed.

Although binder addition is necessary to obtain CPs with suitable flexibility, in order to confirm the fact that the deactivation of the zeolitic CP occurred by the partial encapsulation of the zeolitic material, another catalytic CP was prepared, in the same way as described for the preparation of Pt-NaYZ-P, but without the incorporation of borate (denoted as Pt-NaYZ-PWB). This catalytic CP, Pt-NaYZ-PWB, when evaluated for the test reaction, exhibited a better behavior than the corresponding paper prepared with borate (Pt-NaYZ-P). In this way, the corresponding CO oxidation profile shifted to lower temperatures. Nevertheless, the activity was not the same as that presented for either Pt-NaYZ or Pt-NaYZ-M. To confirm the deactivation of Pt-NaYZ-P by the partial encapsulation of zeolite by the sintering of borates, a powder mechanical mixture of catalyst Pt-NaYZ and anhydrous ulexite ($NaCaB_5O_9$) in the same proportion as in the preparation paste (1/3 wt/wt ratio) was milled in a mortar, calcined at 650 °C for 2 h (denoted as Pt-NaYZ-B), and evaluated for the CO oxidation reaction. Catalytic results demonstrate that it was not possible to reach the same behavior as that of the Pt-NaYZ powder catalyst, confirming the partial blocking of Pt-NaYZ active sites by borate sintering (Fig. 12). As a matter of fact, although Pt could not be detected by EDX (Fig. 8), the activity of the catalyst is directly related to the presence of the noble metal.

It has to be pointed out that all catalytic tests shown in Figs. 10 and 12 were carried out considering the same amount of Pt-NaYZ. It implies that the shift in the light-off curves exhibited for catalytic CPs prepared by the incorporation of the faujasite material during paper manufacturing (Pt-NaYZ-P) is caused by both the partial blocking of zeolite particles and another cause. As retention is an important factor to be considered during paper manufacturing, we intended to prepare a catalytic CP where it can be ensured that all faujasite materials would be retained in the paper structure. To achieve this, a catalytic CP was prepared incorporating Pt-NaYZ by spray (Pt-NaYZ-PS), as described in the "Experimental" section, and tested. As shown in Fig. 12, this catalytic CP (Pt-NaYZ-PS) showed the same light-off profile as those of Pt-NaYZ or Pt-NaYZ-M. Moreover, Pt-NaYZ-PS converts 10 % CO at 50 °C,

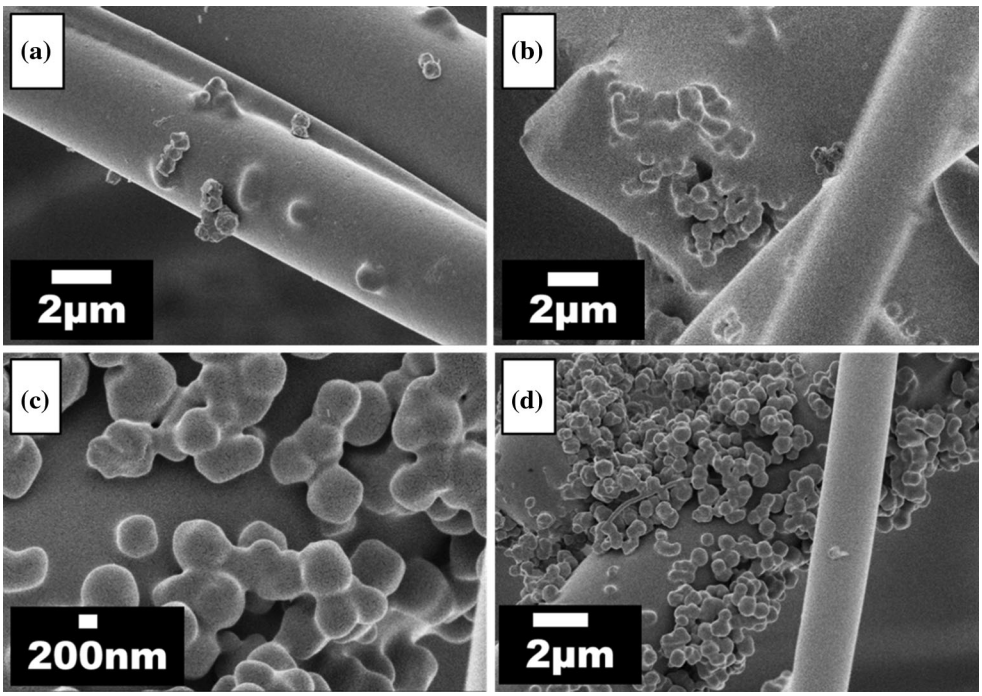

Fig. 11 SEM micrographs showing the partial encapsulation of zeolitic material by borate after calcination of Pt-NaYZ-P

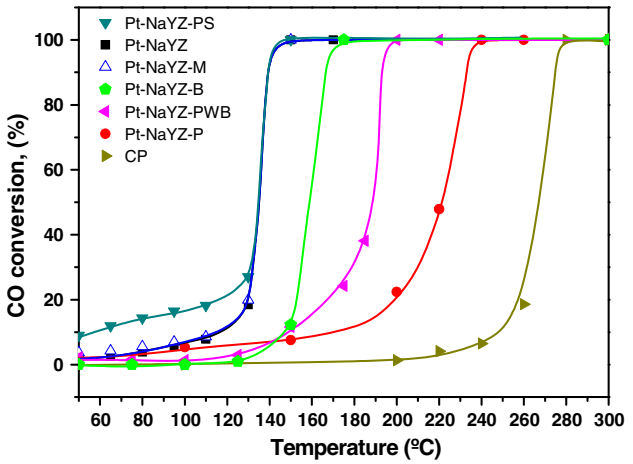

Fig. 12 Recovery of activity of ceramic papers when incorporating the zeolitic material by spray

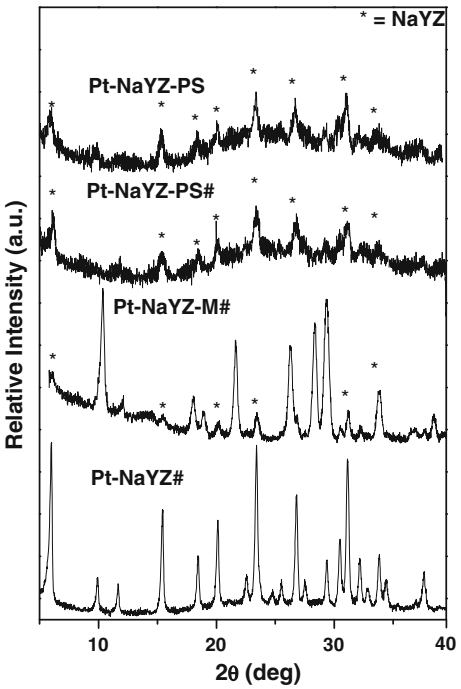

Fig. 13 XRD patterns of catalysts extracted from the reactor after the long-term runs (#). The diffractogram of the sprayed-ceramic paper (Pt-NaYZ-PS) is also included

which indicates that the CP constitutes a good substrate where faujasite particles are well distributed.

Figure 13 (upper curve) shows the XRD pattern of the sprayed-catalytic CP (Pt-NaYZ-PS), where peaks corresponding to Pt-NaYZ can be clearly observed. Figure 14 (a, b) shows the corresponding SEM images. Zeolitic aggregates appear as deposits on ceramic fibers, whereas borate particles join them. Despite its low concentration, Pt could be detected on these zeolitic aggregates in a Pt/Al atomic ratio of < 0.03, which was not the case of the catalytic CPs prepared by incorporating zeolite during the papermaking process (Fig. 3; Table 1).

The catalytic stabilities of Pt-NaYZ, Pt-NaYZ-M, and Pt-NaYZ-PS were checked by carrying out long-term

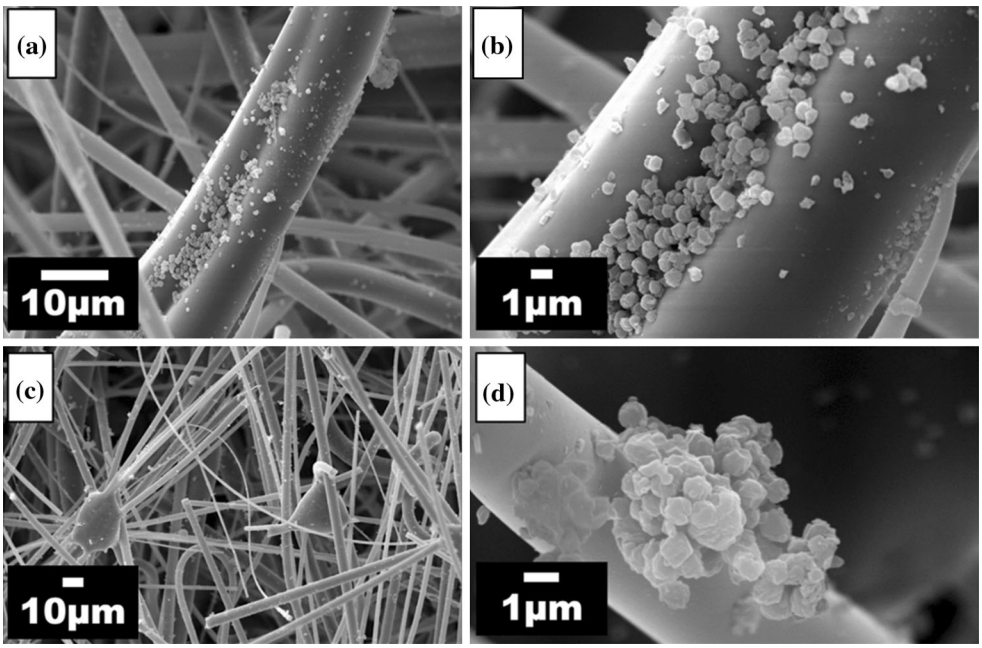

Fig. 14 Morphology of the sprayed-catalytic ceramic paper (Pt-NaYZ-PS) showing zeolitic aggregates before (**a**, **b**) and after (**c**, **d**) the long-term runs

experiments. For this purpose, the catalytic evaluation of these three catalysts was repeated, preparing new batches of catalysts to this end. The catalysts were kept at 150 °C under reaction conditions for more than 90 h. The corresponding curves for these long-term experiments are not shown, since flat profiles were obtained when plotting CO conversion versus time, i.e., the total CO conversion was maintained for all these catalysts, which highlights their catalytic stabilities. Similar results were obtained as new batches of catalysts (Pt-NaYZ, Pt-NaYZ-M, and Pt-NaYZ-PS) were used for these long-term experiments, which demonstrate the reproducibility of the preparation method.

All samples extracted from the reactor after the stability runs, which were denoted as Pt-NaYZ#, Pt-NaYZ-M#, and Pt-NaYZ-PS#, were analyzed by XRD, EDX, and SEM. XRD revealed that no modification of the faujasite was observed for any of the samples studied (powder, monolith, and paper, see Fig. 3 and Fig. 13). The same occurred with the catalyst morphology. Figure 14 shows micrographs for Pt-NaYZ-PS (Fig. 14a, b) and Pt-NaYZ-PS# (Fig. 14c, d). As can be observed, the size and shape of zeolitic aggregates are preserved, which causes the high activity and stability of this sprayed-catalytic paper. Indeed, EDX also revealed the same Pt contents of Pt-NaYZ-PS# and of the fresh (non-evaluated) sample, Pt-NaYZ-PS (Pt/Al atomic ratio <0.03).

As presented above, the way of incorporating the zeolitic component to CPs has to be improved. However, the novelty of using borate compounds as binder components instead of the colloidal commercial components typically employed opens an interesting line of research.

Conclusions

- It was possible to prepare flexible CPs using a natural boron compound (anhydrous ulexite) as binder.
- Zeolitic CPs were obtained incorporating Pt-NaY zeolite either during the papermaking process or by spraying a zeolitic suspension on CPs, the first ones becoming less active toward the CO oxidation reaction due to the partial encapsulation of the faujasite by the sintering of the borate compound during the calcination step.
- Light-off curves indicated that the best performances of the developed structured catalysts were obtained for the rigid system, in which Pt-NaY zeolite was synthesized on cordierite monolith walls as well as for the flexible system, when incorporating the zeolitic component by spray. For both cases, the CO oxidation reaction proceeded at ca. 130 °C, and the total CO conversion was achieved at 150 °C.
- Long-term runs indicated that after more than 90 h under reaction conditions at 150 °C, no deactivation was observed, thus confirming the high catalytic stability of the Pt-NaY zeolite as powder, covering the cordierite monolith walls or sprayed over a catalytic CP.

– Although the retention of inorganic components during the papermaking process was acceptable (higher than 80 %), Pt-NaY zeolite was partially lost during CP manufacturing. This point was solved by spraying zeolite to CP, but the retention during paper preparation needs to be enhanced.

Acknowledgements The authors wish to acknowledge the financial support received from ANPCyT, CONICET, SECTEI Santa Fe government, and UNL. Thanks are also offered to Román Suarez and Rubén Tarcaya from BORAX S.A. for the borates, and to Elsa Grimaldi for the English language editing.

References

1. Nijhuis TA, Beers AEW, Vergunst T, Hoek I, Kapteijn F, Moulijn JA (2001) Preparation of monolithic catalysts. Catal. Rev 43:345–380
2. Patcas FC, Garrido GI, Kraushaar-Czarnetzki B (2007) CO oxidation over structured carriers: a comparison of ceramic foams, honeycombs and beads. Chem Eng Sci 62:3984–3990
3. Shiratori Y, Quang-Tuyen T, Sasaki K (2013) Performance enhancement of biodiesel fueled SOFC using paper-structured catalyst. Int J Hydrog Energy 38:9856–9866
4. Shiratori Y, Ogura T, Nakajima H, Sakamoto M, Takahashi Y, Wakita Y, Kitaoka T, Sasaki K (2013) Study on paper-structured catalyst for direct internal reforming SOFC fueled by the mixture of CH_4 and CO_2. Int J Hydrog Energy 38:10542–10551
5. Shiratori Y, Quang-Tuyen T, Umemura Y, Kitaoka T, Sasaki K (2013) Paper-structured catalyst for the steam reforming of biodiesel fuel. Int J Hydrog Energy 38:11278–11287
6. Bortolozzi JP, Banús ED, Terzaghi D, Gutierrez LB, Milt VG, Ulla MA (2013) Novel catalytic ceramic papers applied to oxidative dehydrogenation of ethane. Catal Today 216:24–29
7. Miura S, Umemura Y, Shiratori Y, Kitaoka T (2013) In situ synthesis of Ni/MgO catalysts on inorganic paper-like matrix for methane steam reforming. Chem Eng J 229:515–521
8. Koga H, Kitaoka T, Nakamura M, Wariishi H (2009) Influence of a fiber-network microstructure of paper-structured catalyst on methanol reforming behavior. J Mater Sci 44:5836–5841. doi:10.1007/s10853-009-3823-y
9. Koga H, Kitaoka T (2011) One-step synthesis of gold nanocatalysts on a microstructured paper matrix for the reduction of 4-nitrophenol. Chem Eng J 168:420–425
10. Koga H, Umemura Y, Kitaoka T (2011) Design of catalyst layers by using paper-like fiber/metal nanocatalyst composites for efficient NO_X reduction. Compos B 42:1108–1113
11. Koga H, Ishihara H, Kitaoka T, Tomoda A, Suzuki R, Wariishi H (2010) NO_X reduction over paper-structured fiber composites impregnated with Pt/Al_2O_3 catalyst for exhaust gas purification. J Mater Sci 45:4151–4157. doi:10.1007/S10853-010-4504-6
12. Cecchini JP, Serra RM, Barrientos CM, Ulla MA, Galván MV, Milt VG (2011) Ceramic papers containing Y zeolite for toluene removal. Microporous Mesoporous Mater 145:51–58
13. Tuler FE, Banús ED, Zanuttini MA, Miró EE, Milt VG (2014) Ceramic papers as flexible structures for the development of novel diesel soot combustion catalysts. Chem Eng J 246:287–298
14. Ichiura H, Okamura N, Kitaoka T, Tanaka H (2001) Preparation of zeolite sheet using a papermaking technique, zeolite sheet and its hygroscopic characteristics. J Mater Sci 36:4921–4926. doi:10.1023/A:1011840405043
15. Cecchini JP, Serra R, Ulla MA, Zanuttini MA, Milt VG (2013) Enhancing mechanical properties of ceramic papers loaded with zeolites using borate compound as binders. Bioresources 8:313–326
16. http://minerals.stage.riotintodev.com/documents/RTM.SiteMap.Sept2011.pdf
17. Oran U, Uner D (2004) Mechanisms of CO oxidation reaction and effect of chlorine ions on the CO oxidation reaction over Pt/CeO_2 and Pt/CeO_2/γ-Al_2O_3 catalysts. Appl Catal B 54:183–191
18. Kulshreshtha SK, Sharma S, Vijayalakshmi R, Sasikala R (2004) CO oxidation over Pd/γ- $FeMnO_3$ catalyst, indian. J Chem Technol 11:427–433
19. Immamura S, Tsuji Y, Miyake Y, Ito T (1995) Cooperative action of palladium and manganese (III) oxide in the oxidation of carbon monoxide. J Catal 151:279–284
20. Comotti M, Li W-C, Spliethoff B, Schuth F (2006) Support effect in high activity gold catalysts for CO oxidation. J Am Chem Soc 128:917–924
21. Lepage M, Visser T, Soulimani F, Beale AM, Iglesias-Juez A, van der Eerden AMJ, Weckhuysen BM (2008) Promotion effects in the oxidation of CO over zeolite-supported Rh nanoparticles. J Phys Chem C 112:9394–9404
22. Han W, Zhang P, Tang Z, Lu G (2013) Low temperature CO oxidation over Pd–Ce catalysts supported on ZSM-5 zeolites, Process Saf Environ. doi:10.1016/j.psep.2013.04.003
23. Astudillo J, Águila G, Díaz F, Guerrero S, Araya P (2010) Study of CuO–CeO_2 catalysts supported on SiO_2 on the low-temperature oxidation of CO. Appl Catal A 381:169–176
24. Todorova S, Kadinov G, Tenchev K, Caballero A, Holgado JP, Pereñiguez R (2009) Co_3O_4 + CeO_2/SiO_2 Catalysts for n-Hexane and CO Oxidation. Catal Lett 129:149–155
25. Xu J, Xu X, Ouyang L, Yang X, Mao W, Su J, Han Y (2012) Mechanistic study of preferential CO oxidation on a Pt/NaY zeolite catalyst. J Catal 287:114–123
26. Banús ED, Milt VG, Miró EE, Ulla MA (2010) Co, Ba, K/ZrO_2 coated onto metallic foam (AISI 314) as a structured catalyst for soot combustion: coating preparation and characterization. Appl Catal A 379:95–104
27. Banús ED, Milt VG, Miró EE, Ulla MA (2009) Structured catalyst for the catalytic combustion of soot: Co, Ba, K/ZrO_2 supported on Al2O3 foam. Appl Catal A 362:129–138
28. Banús ED, Milt VG, Miró EE, Ulla MA (2013) Catalytic coating synthesized onto cordierite monolith walls. Its application to diesel soot combustion. Appl Catal B 132–133:479–486
29. Milt VG, Ivanova S, Sanz O, Domínguez MI, Corrales A, Odriozola JA, Centeno MA (2013) Au/TiO_2 supported on ferritic stainless steel monoliths as CO oxidation catalysts. Appl Surf Sci 270:169–177
30. Pérez NC, Miró EE, Zamaro JM (2013) Cu, Ce/mordenite coatings on FeCrAl-alloy corrugated foils employed as catalytic microreactors for CO oxidation. Catal Today 213:183–191
31. Huang Q, Yan X, Li B, Xu X, Chen Y, Zhu S, Shen S (2013) Activity and stability of Pd/$MMnO_x$ (M = Co, Ni, Fe and Cu) supported on cordierite as CO oxidation catalysts. J Ind Eng Chem 19:438–443
32. Domínguez MI, Sánchez M, Centeno MA, Montes M, Odriozola JA (2006) CO oxidation over gold-supported catalysts-coated ceramic foams prepared from stainless steel wastes. Appl Catal A 302:96–103
33. Bortolozzi JP, Banús ED, Gutierrez LB, Ulla MA (2011) Pt/Al_2O_3 structured catalyst onto a stainless steel (AISI 314) foam for CO oxidation. ACI 2(3):79–87
34. Pérez NC, Miró EE, Zamaro JM (2013) Microreactors based on CuO–CeO_2/zeolite films synthesized onto brass microgrids for the oxidation of CO. Appl Catal B 129:416–425

35. Baimpos T, Kouzoudis D, Gora L, Nikolakis V (2011) Are zeolite films flexible? Chem Mater 23:1347–1349
36. Prasad R, Singh P (2012) A review on CO oxidation over copper chromite catalyst. Catal Rev 54:224–279
37. Ichiura H, Kubota Y, Wu Z, Tanaka H (2001) Preparation of zeolite sheets using a papermaking technique Part I dual polymer system for high retention of stock components. J Mater Sci 36:913–917. doi:10.1023/A:1004851101749